

Mid-infrared luminescence of Dy^{3+}-doped Ga_2S_3-Sb_2S_3-CsI chalcohalide glasses

Anping Yang(杨安平), Jiahua Qiu(邱嘉桦), Mingjie Zhang(张鸣杰), Mingyang Sun(孙明阳), Zhiyong Yang(杨志勇)

Citation: Chin. Phys. B . 2018, 27(7): 077105. **doi:** 10.1088/1674-1056/27/7/077105

Journal homepage: http://cpb.iphy.ac.cn; http://iopscience.iop.org/cpb

What follows is a list of articles you may be interested in

Electronic structure and magnetic properties of rare-earth perovskite gallates from first principles

A Dahani, H Alamri, B Merabet, A Zaoui, S Kacimi, A Boukortt, M Bejar

Chin. Phys. B . 2017, 26(1): 017101. **doi:** 10.1088/1674-1056/26/1/017101

Band-gap engineering of $La_{1-x}Nd_xAlO_3$ (x = 0, 0.25, 0.50, 0.75, 1) perovskite using density functional theory: A modified Becke Johnson potential study

Sandeep, D P Rai, A Shankar, M P Ghimire, Anup Pradhan Sakhya, T P Sinha, R Khenata, S Bin Omran, R K Thapa

Chin. Phys. B . 2016, 25(6): 067101. **doi:** 10.1088/1674-1056/25/6/067101

Homopolar bonds in Se-rich Ge—As—Se chalcogenide glasses

Si-Wei Xu(许思维), Rong-Ping Wang(王荣平), Zhi-Yong Yang(杨志勇), Li Wang(王丽), Luther-Davies Barry

Chin. Phys. B . 2016, 25(5): 057105. **doi:** 10.1088/1674-1056/25/5/057105

Tb doping induced enhancement of anomalous Hall effect in NiFe films

Zhu Jia-Peng, Ma Li, Zhou Shi-Ming, Miao Jun, Jiang Yong

Chin. Phys. B . 2015, 24(1): 017101. **doi:** 10.1088/1674-1056/24/1/017101

A first-principles study of B2 NiAl alloyed with rare earth element Pr, Pm, Sm, and Eu

He Jun-Qi, Wang You, Yan Mu-Fu, Pan Zhao-Yi, Guo Li-Xin

Chin. Phys. B . 2013, 22(2): 027102. **doi:** 10.1088/1674-1056/22/2/027102

Mid-infrared luminescence of Dy^{3+}-doped Ga_2S_3–Sb_2S_3–CsI chalcohalide glasses*

Anping Yang(杨安平)[1], Jiahua Qiu(邱嘉桦)[1], Mingjie Zhang(张鸣杰)[1,2], Mingyang Sun(孙明阳)[1], and Zhiyong Yang(杨志勇)[1,†]

[1] *Jiangsu Key Laboratory of Advanced Laser Materials and Devices, School of Physics and Electronic Engineering, Jiangsu Normal University, Xuzhou* 221116, *China*

[2] *State Key Laboratory of Silicate Materials for Architectures, Wuhan University of Technology, Wuhan* 430070, *China*

(Received 24 January 2018; revised manuscript received 30 March 2018; published online 25 June 2018)

The mid-infrared (MIR) luminescent properties of Dy^{3+} ions in a new chalcohalide glass host, Ga_2S_3–Sb_2S_3–CsI, are investigated; and the suitability of the doped glass for MIR fiber lasers is evaluated. The Dy^{3+}-doped chalcohalide glasses exhibit good thermal stability and intense MIR emissions around 2.96 μm and 4.41 μm. These emissions show quantum efficiencies (η) as high as ~ 60%, and have relatively large stimulated emission cross sections (σ_{em}). The low phonon energy (~ 307 cm^{-1}) of the host glass accounts for the intense MIR emissions, as well as the high η. These favorable thermal and emission properties make the Dy^{3+}-doped Ga_2S_3–Sb_2S_3–CsI glasses promising materials for MIR fiber amplifiers or lasers.

Keywords: chalcogenide glasses, rare earth, emission property, mid-infrared laser

PACS: 71.23.Cq, 76.30.Kg, 78.45.+h, 95.85.Hp **DOI:** 10.1088/1674-1056/27/7/077105

1. Introduction

Mid-infrared (MIR) lasers are quite useful light sources for gas sensing, chemical process monitoring, military and medical applications.[1–5] Various active gain media operating in 2–5 μm wavelength region have been extensively studied including rare earth (RE) ions doped glass fibers[1,6,7] and crystals,[8–10] transition metal (TM) doped crystals,[4] and so on. For example, Pr^{3+} ions doped $LaCl_3$ crystal has exhibited the longest wavelength of 7.2 μm laser output at room temperature so far; laser outputs in the wavelength ranges of 1.8–3.1 μm and 3.9–5.1 μm have been achieved in Cr^{2+}: ZnSe and Fe^{2+}: ZnSe crystals, respectively. However, the crystals suffer from the long growth cycle, complex preparation techniques, and relatively high cost, which restrict their practical applications. In comparison, glass media are known for ease of large-scale and complex shape production, wide tuning range of compositions, as well as superior chemical and mechanical durability. Continuous wave (CW) lasings at 2.8 μm, 2.9 μm, and 3.5 μm have been obtained in Er^{3+} and Ho^{3+} ions doped ZBLAN glass fibers at room temperature, but it remains highly challenging for lasing at longer wavelengths.

Due to the outstanding MIR transmitting property and low phonon energy of chalcogenide glass (ChG), RE ions doped ChGs are considered to be ideal candidates as MIR laser gain materials. Recently, an increasing number of studies focused on the MIR emission characteristics of RE ions in ChGs.[11–18] Among the RE ions, Dy^{3+} represents a typical three-level lasing system with an emission peak locating at ~ 3 μm that can be pumped to the $^6H_{11/2}$ excited state by ~ 1.7 μm light. The simple and effective energy level structure of Dy^{3+} facilitates the development of amplifiers or lasers operating at ~ 3 μm.[19] Moreover, Dy^{3+} ions are also potentially feasible for the ~ 4.4 μm MIR emission, which is extremely difficult if not entirely impossible to be realized in other glass hosts because of the strong luminescence quenching related to the high multi-phonon relaxation (MPR) rate. Recently, Ga_2S_3–Sb_2S_3–CsI chalcohalide glasses[20] stand out as promising MIR laser gain media owing to the outstanding properties including low phonon energy, large solubility of RE ions, and good thermal stability. In this work, the thermal stability, structure and MIR luminescent properties of Dy^{3+}-doped Ga_2S_3–Sb_2S_3–CsI chalcohalide glasses were studied, and their suitability for MIR fiber lasers was assessed.

2. Experimental procedures

In this study, the composition 20 Ga_2S_3–60 Sb_2S_3–20 CsI,[20] which has optimized thermal stability against crystallization in the chalcohalide system, was chosen as the host glass. The RE doped glasses, $(20-x)$ Ga_2S_3–60 Sb_2S_3–20 CsI–x Dy_2S_3 ($x = 0$, 0.05, 0.20, 0.40, 0.80, 1.00, 1.20), were synthesized through a melt-quenching method. High purity Sb (6N), Ga (6N), S (6N), CsI (5N), and Dy_2S_3 (3N) were

*Project supported by the National Natural Science Foundation of China (Grant Nos. 61405080 and 61575086), Jiangsu Collaborative Innovation Centre of Advanced Laser Technology and Emerging Industry, China, and the Priority Academic Program Development of Jiangsu Higher Education Institutions, China.

†Corresponding author. E-mail: yangzhiyong@jsnu.edu.cn

© 2018 Chinese Physical Society and IOP Publishing Ltd

weighed and loaded in a silica tube with an inner diameter of 9 mm. The tube containing the mixture was subsequently evacuated down to less than 10^{-5} mbar. The mixture was then baked at 100 °C for more than 2 h to reduce possible moisture. After that, the tube was sealed and heated to 950 °C in a rocking furnace. The mixture was homogenized at this temperature for more than 12 h. In the end, the tube was quenched in water, and the formed glass was annealed to reduce the internal stress.

The differential scanning calorimetry (DSC) curves were measured by a TA Q2000 calorimeter. About 5–15 mg glass was used for each measurement, and the heating rate was 10 °C/min. The transmission spectra in 0.5–3.3 μm were measured using a Perkin–Elmer Lambda 950 spectrophotometer and those in 3.3–20 μm were recorded with a Bruker Tensor 27 IR spectrophotometer. The refractive indices were tested by a Woollam IR-VASE ellipsometer.[21,22] The MIR emission spectra and corresponding lifetimes were recorded with an Edinburgh FS980 fluorescence spectrometer. The measurement details are similar to those described in Ref. [11]. To measure the Raman spectra, a customized BWTek BWS415 Raman spectrometer with an excitation wavelength of 785 nm was used.

3. Results

To investigate the impact of Dy^{3+} dopant on the thermal stability of the Ga_2S_3–Sb_2S_3–CsI chalcohalide glasses, the glass transition temperature (T_g) and the onset crystallization temperature (T_x) are determined based on the measured DSC curves and listed in Table 1. The T_g increases slightly with increasing amount of Dy^{3+} dopant. The ΔT ($= T_x$–T_g), a measure of the thermal stability against crystallization, is larger than 100 °C, pointing to the good thermal stability of the prepared glasses.

Table 1. Characteristic temperatures of $(20-x)$ Ga_2S_3–60 Sb_2S_3–20 CsI–x Dy_2S_3 glasses.

x	T_g/°C	T_x/°C	ΔT/°C
0	228 ± 1	361 ± 1	133
0.05	229 ± 1	357 ± 1	128
0.20	231 ± 1	343 ± 1	112
0.40	232 ± 1	348 ± 1	116
0.80	233 ± 1	340 ± 1	107
1.00	234 ± 1	337 ± 1	103
1.20	235 ± 1	350 ± 1	115

Figure 1 displays the absorption spectra of the Dy^{3+}-doped Ga_2S_3–Sb_2S_3–CsI chalcohalide glasses in the wavelength range of 0.5–3.3 μm. Six absorption bands centered at 0.81 μm, 0.92 μm, 1.11 μm, 1.30 μm, 1.70 μm, and 2.85 μm are observed. These bands are attributed to the 4f–4f electron transitions of Dy^{3+} from its ground level $^6H_{15/2}$ to the excited ones, which are displayed in the figure. In the absorption spectra, the intensity at 1.30 μm is the strongest, indicating that the glasses can be efficiently excited by ∼ 1.30 μm light.

Based on the absorption spectra, the emission spectra of the $(20-x)$ Ga_2S_3–60 Sb_2S_3–20 CsI–x Dy_2S_3 chalcohalide glasses in the 2–5 μm MIR range were measured using a 1.32 μm CW semiconductor laser as the excitation light source (see Fig. 2). Three strong emission bands centered at 2.45 μm, 2.96 μm, and 4.41 μm are observed. These bands correspond to the transitions $^6H_{9/2}$, $^6F_{11/2} \rightarrow {}^6H_{13/2}$, $^6H_{13/2} \rightarrow {}^6H_{15/2}$, and $^6H_{11/2} \rightarrow {}^6H_{13/2}$, respectively. The emission intensities (EIs) increase with the increasing amount of Dy^{3+} dopant until the doping level reaches ∼ 0.36 mol% ($x = 0.8$), where the doped glass shows the strongest emissions. When the Dy^{3+} concentration is higher than 0.36 mol%, the EIs reduce with increasing doping content. This is associated with the concentration quenching effect,[23] which usually happens at high doping concentrations and tends to overwhelm the radiative transitions.

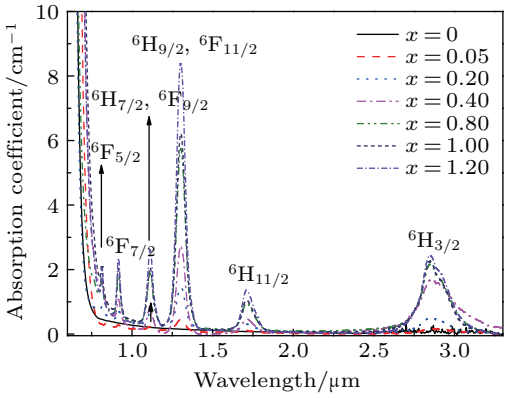


Fig. 1. (color online) Absorption spectra of $(20-x)$ Ga_2S_3–60 Sb_2S_3–20 CsI–x Dy_2S_3 glasses.

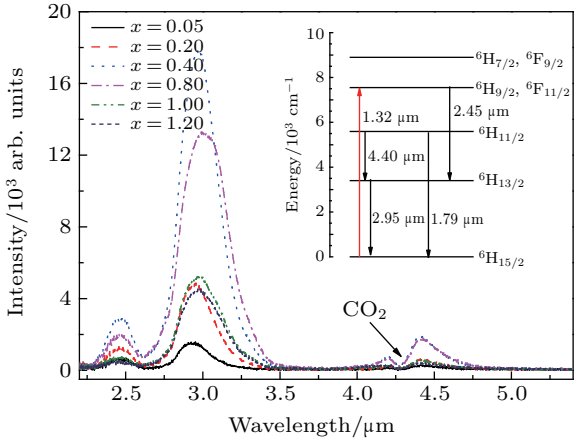


Fig. 2. (color online) MIR emission spectra of $(20-x)$ Ga_2S_3–60 Sb_2S_3–20 CsI–x Dy_2S_3 glasses when excited at 1.32 μm, the inset shows possible transitions between energy levels of Dy^{3+}.

To reveal the underlying structural influence on the luminescence properties of the dopant, the structure of the host

glass was studied by Raman spectroscopy. Figure 3 displays the reduced Raman[24] spectrum of 20 Ga_2S_3–60 Sb_2S_3–20 CsI (Ga–Sb–S–CsI or GSSC) glass. As a comparison, the Raman spectrum of 20 Ga_2S_3–60 Ge_2S_3–20 CsI (Ga–Ge–S–CsI or GGSC) glass was also measured and shown in Fig.3. For the GSSC glass, the main Raman band peaking at 330 cm^{-1} can be deconvoluted into three Gaussian sub-bands corresponding to the vibrations of S_3Ga–GaS_3 ($\sim$ 265 cm^{-1}),[25,26] [SbS_3] ($\sim$ 314 cm^{-1}),[27,28] and [GaS_4] ($\sim$ 342 cm^{-1}) structural units.[25,29] As to the GGSC glass, the Raman band consists of vibrations ascribed to $S_3Ga(Ge)$–$Ga(Ge)S_3$ ($\sim$ 265 cm^{-1}),[30] [GaS_3I] ($\sim$ 296 cm^{-1}),[31] corner-sharing [$Ga(Ge)S_4$] ($\sim$ 342 cm^{-1}, 390 cm^{-1}, 425 cm^{-1}),[25,29,32] edge-sharing [$Ga(Ge)S_4$] ($\sim$ 370 cm^{-1}) and S–S (438 cm^{-1}) structural units (see Fig. 3). Based on the Raman shifts and integral areas of the sub-bands, the effective phonon energies (EPEs) are estimated to be 307 cm^{-1} and 352 cm^{-1} for the GSSC and GGSC glasses, respectively. The lower EPE of the GSSC glass would result in smaller MPR rates for the doping RE ions, and therefore improve the MIR luminescent properties of the RE ions in the glass.

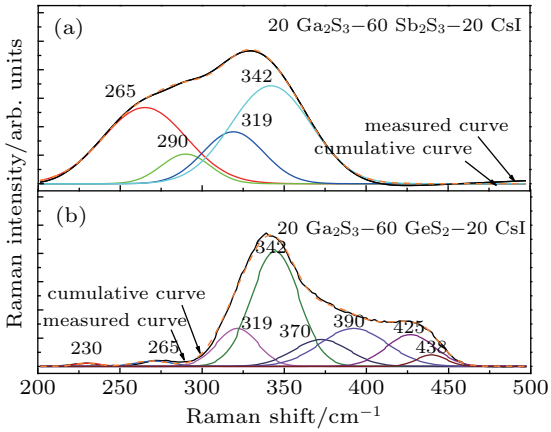


Fig. 3. (color online) Reduced Raman spectra of (a) 20 Ga_2S_3–60 Sb_2S_3–20 CsI and (b) 20 Ga_2S_3–60 GeS_2–20 CsI glasses.

4. Discussion

To assess the suitability of the Dy^{3+}-doped GSSC glasses as MIR gain media, we conducted a Judd–Ofelt (J–O)[33,34] analysis on the glasses according to the absorption spectra (see Fig. 1) and calcluated associated radiative parameters. Table 2 displays the experimental (f_{exp}) and calculated (f_{cal}) oscillator strengths of the considered transitions. The absorption band at 2.85 μm was excluded in the calculation because the OH impurity also has contrubition to this band. The J–O intensity parameters obtained by fitting the f_{exp} are $\Omega_2 = 10.73 \times 10^{-20}$ cm^2, $\Omega_4 = 3.18 \times 10^{-20}$ cm^2, and $\Omega_6 = 1.53 \times 10^{-20}$ cm^2. Using the J–O intensity parameters, we calculated the radiative parameters related to the MIR emissions of Dy^{3+} ions (see Table 3). The equations used in the calculations can be found in Refs. [35] and [36]. The 2.96 μm and 4.41 μm emissions possess quantum efficiencies (η) of $\sim$ 61.0% and $\sim$ 58.0%; and the corresponding stimulated emission cross sections (σ_{em}) are $\sim 1.04 \times 10^{20}$ cm^2 and $\sim 0.27 \times 10^{20}$ cm^2, respectively. As a comparison, the η and corresponding σ_{em} for the emissions of Dy^{3+} in a few other ChGs are also shown in Table 3. The η of the MIR emissions in Dy^{3+}-doped GSSC glass is obviously larger than that of the corresponding emissions in Dy^{3+}-doped GGSC, Ga–Ge–S, Ga–Ge–S–CdI, and Ga–La–S glasses. The high η is associated with the low EPE of the GSSC glass. It is worth mentioning that the η of the MIR emissions in Dy^{3+}-doped GSSC glass is lower than that in Dy^{3+}-doped Ga–Sb–S glass, although the two hosts have almost the same EPE.[37] This may be caused by the higher OH content in the former glass. CsI is moisture sensitive and tends to bring additional OH impurity into the glass. Figure 4 shows the IR transmission spectra of 20 Ga_2S_3–60 Sb_2S_3–20 CsI and 20 Ga_2S_3–80 Sb_2S_3 glasses prepared at the same condition. It is clear that the addition of CsI indeed brings more OH impurity into the glass as reflected by the stronger absorption band around 2.9 μm. The OH impurity has been known to have a significant quenching effect on the MIR fluorescence.[38,39] This situation can also explain the remarkable η difference between Dy^{3+}-doped Ga–Ge–S and Ga–Ge–S–CsI glasses (see Table 3). The OH content might be greatly reduced if appropriate purification processes are applied during the glass synthesis. Thus, the η of the MIR emissions could be further improved. The σ_{em} of the MIR emissions of Dy^{3+} in GSSC glass is also relatively large, which is beneficial to the material for achieving high gain factor.[40] Figure 5 further compares the 2–5 μm emissions of 0.36 mol% Dy^{3+} doped GSSC and GGSC glasses. The former shows much stronger emissions than the latter, which is consistent with the lower-phonon-energy feature of the former. The high η and large σ_{em} for the MIR emissions in the Dy^{3+}-doped GSSC glasses demonstrate their suitability for MIR fiber amplifiers or lasers.

Table 2. Experimental (f_{exp}) and calculated (f_{cal}) oscillator strengths of electron transitions for 19.2 Ga_2S_3–60 Sb_2S_3–20 CsI–0.8 Dy_2S_3 glass. λ and δ are wavelength and deviation of f_{exp} from f_{cal}, respectively.

Transition	λ /nm	$f_{exp}/10^{-6}$	$f_{cal}/10^{-6}$	$\delta/10^{-6}$
$^6H_{15/2} \rightarrow {}^6F_{7/2}$	918	3.75	3.23	0.52
$^6H_{15/2} \rightarrow {}^6H_{7/2}+{}^6F_{9/2}$	1113	5.31	5.39	–0.08
$^6H_{15/2} \rightarrow {}^6H_{9/2}+{}^6F_{11/2}$	1302	20.00	19.92	0.08
$^6H_{15/2} \rightarrow {}^6H_{11/2}$	1710	1.84	2.06	–0.22

Table 3. Radiative parameters of Dy^{3+} ions in various hosts. λ, n, β, τ_{rad}, τ_{mea}, η, and σ_{em} are the wavelength, refractive index, fluorescence branch ratio, radiative lifetime, measured fluorescence lifetime, quantum efficiency, and stimulated emission cross section, respectively.

Host glass	Transition	λ/μm	n	β/%	τ_{rad}/ms	τ_{mea}/ms	η/%	$\sigma_{em}/10^{20}$ cm^2	Ref.
Ga–Sb–S–CsI	$^6H_{11/2} \rightarrow {}^6H_{13/2}$	4.41	2.444 ± 0.001	16	2.50	1.45 ± 0.02	58.0	0.27	this work
	$^6H_{13/2} \rightarrow {}^6H_{15/2}$	2.96	2.454 ± 0.001	100	5.19	3.17 ± 0.02	61.0	1.04	this work
Ga–Ge–S–CsI	$^6H_{11/2} \rightarrow {}^6H_{13/2}$	4.41	1.991 ± 0.001	16	3.94	1.02 ± 0.02	26.0		this work
	$^6H_{13/2} \rightarrow {}^6H_{15/2}$	2.96	1.996 ± 0.001	100	8.18	2.31 ± 0.02	28.0		this work
Ga–Sb–S	$^6H_{11/2} \rightarrow {}^6H_{13/2}$	4.40	2.69	14	1.87	1.42	75.9	0.38	[13]
	$^6H_{13/2} \rightarrow {}^6H_{15/2}$	2.95	2.72	100	4.11	3.62	88.1	1.11	[13]
Ga–Ge–S	$^6H_{11/2} \rightarrow {}^6H_{13/2}$	4.40	2.08	14.4	3.17	1.31	41.3	0.36	[13]
	$^6H_{13/2} \rightarrow {}^6H_{15/2}$	2.95	2.10	100	6.99	3.53	50.5	0.86	[13]
Ga–Ge–S–CdI	$^6H_{11/2} \rightarrow {}^6H_{13/2}$	4.40	–	15	3.63	–	–	0.19[a)]	[15]
	$^6H_{13/2} \rightarrow {}^6H_{15/2}$	2.95		100	8.20	0.86	10.5	0.84	[15]
Ga–La–S	$^6H_{11/2} \rightarrow {}^6H_{13/2}$	4.40		14	2.53	1.3	51.4		[41]
	$^6H_{13/2} \rightarrow {}^6H_{15/2}$	2.95	2.4	100	6.29	3.6	57.2	0.92	[41]

[a)] this value is recalculated by taking β into account.

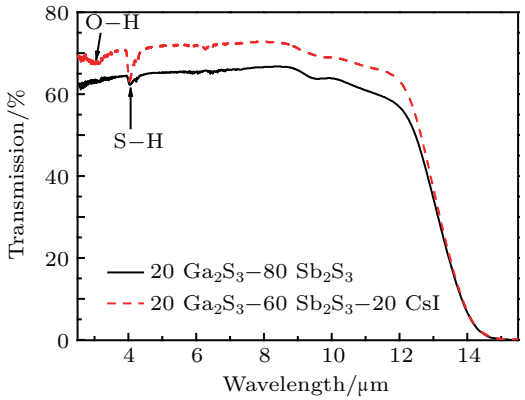


Fig. 4. (color online) Transmission spectra of 20 Ga_2S_3–80 Sb_2S_3 and 20 Ga_2S_3–60 Sb_2S_3–20 CsI glasses (thickness = 2.1 mm).

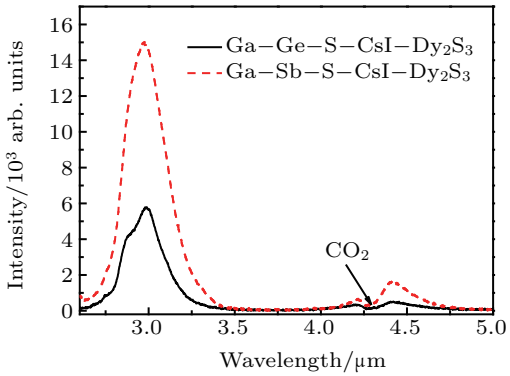


Fig. 5. (color online) The 2.5–5 μm emission spectra of Ga–Sb–S–CsI and Ga–Ge–S–CsI glasses doped with 0.36 mol% Dy^{3+} ions.

5. Conclusion

The $(20-x)$ Ga_2S_3–60 Sb_2S_3–20 CsI–x Dy_2S_3 ($x = 0$, 0.05, 0.20, 0.40, 0.80, 1.00, 1.20) chalcohalide glasses have good thermal stability and show intense emissions centered at 2.96 μm and 4.41 μm. The strongest MIR emissions are observed when the concentration of Dy^{3+} ions is 0.36 mol%. The η of the 2.96 μm and 4.41 μm emissions are about 61.0% and 58.0%, and the corresponding σ_{em} are 1.04×10^{-20} cm^2 and 0.27×10^{-20} cm^2, respectively. The high η coupled with the relatively large σ_{em} bode well for the potential of the Dy^{3+}-doped Ga_2S_3–Sb_2S_3–CsI glasses as MIR gain media.

References

[1] Jackson S D 2012 *Nat. Photon.* **6** 423
[2] Kimber J A, Foreman L, Turner B, Rich P and Kazarian S 2016 *Faraday Discuss.* **187** 69
[3] Lucas P, Coleman G, Cantoni C, Jiang S, Luo T, Bureau B, Boussard-Pledel C, Troles J and Yang Z Y 2017 *Proc. SPIE* **10058** 100580Q
[4] Mirov S B, Fedorov V V, Moskalev I S and Martyshkin D V 2007 *IEEE J. Sel. Top. Quant.* **13** 810
[5] Yan T Y, Shen X, Wang R P, Wang G X, Dai S X, Xu T F and Nie Q H 2017 *Chin. Phys. B* **26** 024213
[6] Zhou P, Wang X, Ma Y, Lv H and Liu Z J 2012 *Laser Phys.* **22** 1744
[7] Seddon A B, Tang Z Q, Furniss D, Sujecki S and Benson T M 2010 *Opt. Express* **18** 26704
[8] Bowman S R, Shaw L B, Feldman B J and Ganem J 1996 *IEEE J. Quant. Electron.* **32** 646
[9] Djeu N, Hartwell V E, Kaminskii A A and Butashin A V 1997 *Opt. Lett.* **13** 997
[10] Zhao X Y, Sun D L, Luo J Q, Zhang H L, Fang Z Q, Quan C, Li X L, Cheng M J, Zhang Q L and Yin S T 2017 *Chin. Phys. B* **26** 074217
[11] Hu J, Menyuk C R, Wei C L, Shaw L B, Sanghera J S and Aggarwal I D 2015 *Opt. Lett.* **40** 3687
[12] Charpentier F, Starecki F, Doualan J L, Jóvári P, Camy P, Troles J, Belin S, Bureau B and Nazabal V 2013 *Mater. Lett.* **101** 21
[13] Zhang M J, Yang A P, Peng Y F, Zhang B, Ren H, Guo W, Yang Y, Zhai C C, Wang Y W, Yang Z Y and Tang D Y 2015 *Mater. Res. Bull.* **70** 55
[14] Liu Y Y, Liao M S, Wang X, Chen G R and Hu L L 2017 *J. Lumin.* **187** 1
[15] Wang Z, Guo H, Xiao X, Xu Y, Cui X, Lu M, Peng B, Yang A, Yang Z and Gu S 2017 *J. Alloys Compd.* **692** 1010
[16] Ren J, Chen D P, Yang G, Xu Y S, Zeng H D and Chen G R 2007 *Chin. Phys. Lett.* **24** 1985
[17] Qi J N, Xu Y S, Huang F, Chen L Y, Han Y, Xue B, Zhang S Q, Xu T F and Dai S X 2014 *J. Am. Ceram. Soc.* **97** 1471
[18] Xu Y S, Zhang Q, Shen C, Chen D P, Zeng H D and Chen G R 2009 *J. Am. Ceram. Soc.* **92** 3088
[19] Ren J, Wagner T, Bartos M, Frumar M, Oswald J, Kincl M, Frumarova B and Chen G 2011 *J. Appl. Phys.* **109** 033105
[20] Qiu J H, Yang A P, Zhang M J, Li L, Zhang B, Tang D Y and Yang Z Y 2017 *J. Am. Ceram. Soc.* **100** 5107
[21] Woollam J A, Johs B, Herzinger C M, Hilfiker J, Synowicki R and Bungay C L 1999 *Crit. Rev. Opt. Sci. Technol.* **72** 3
[22] Yang Y, Yang Z Y, Lucas P, Wang Y W, Yang Z J, Yang A P, Zhang B and Tao H Z 2016 *J. Non-Cryst. Solids* **440** 38
[23] Yang Z Y, Li B T, He F, Luo L and Chen W 2008 *J. Non-Cryst. Solids* **354** 1198

[24] Brooker M H, Nielsen O F and Praestgaard E 1988 *J. Raman Spectrosc.* **19** 71

[25] Ichikawa M, Wakasugi T and Kadono K 2010 *J. Non-Cryst. Solids* **356** 2235

[26] Tao H Z, Zhao X J, Jing C B, Yang H and Mao S 2005 *Solid State Commun.* **133** 327

[27] Frumarová B, Němec P, Frumar M, Oswald J and Vlček M 1998 *Semiconductor* **32** 812

[28] Guo H T, Zhang M J, Xu Y T, Xiao X S and Yang Z Y 2017 *Chin. Phys. B* **26** 104208

[29] Heo J, Min Yoon J and Ryou S Y 1998 *J. Non-Cryst. Solids* **238** 115

[30] Mao S, Tao H Z, Zhao X J, Dong G P and Guo H T 2007 *Solid State Commun.* **142** 453

[31] Nakamoto K 2008 *Infrared Raman Spectra Inorg. Coordination Compd. Part. A: Theory Appl. Inorg. Chem.* (6th Edn.) (Hoboken: Wiley) pp. 129–196

[32] Musgraves J D, Wachtel P, Gleason B and Richardson K 2014 *J. Non-Cryst. Solids* **386** 61

[33] Judd B R 1962 *Phys. Rev.* **127** 750

[34] Ofelt G S 1962 *J. Chem. Phys.* **37** 511

[35] Chen D Q, Wang Y S, Yu Y L, Ma E and Hu Z J 2005 *J. Phys.: Condens. Matter* **17** 6545

[36] Yang Z Y, Chen W and Luo L 2005 *J. Non-Cryst. Solids* **351** 2513

[37] Yang A, Zhang M, Li L, Wang Y, Zhang B, Yang Z and Tang D 2016 *J. Am. Ceram. Soc.* **99** 12

[38] Wang X S, Song B A, Zhang W, Dai S X, Wang G X, Xu T F, Shen X, Zhang X H, Liu C, Xu K and Heo J 2011 *J. Non-Cryst. Solids* **357** 2403

[39] Liu X B, Tikhomirov V and Jha A 2000 *J. Mater. Res.* **15** 2864

[40] Lin H, Chen D Q, Yu Y L, Yang A P and Wang Y S 2011 *Opt. Lett.* **36** 1815

[41] Schweizer T, Hewak D W, Samson B N and Payne D N 1996 *Opt. Lett.* **21** 1594